

Decomposing heterogeneity in cure rate models via discrete waring frailty under minimum activation

Abstract

This paper develops a flexible survival model for data with a cure fraction, where the number of latent risk factors follows a Waring distribution under a minimum activation scheme. The primary objective is to provide a framework that more accurately captures and disentangles the distinct sources of heterogeneity, namely internal (individual susceptibility) and external (unobserved covariates), often confounded in traditional cure rate models. While models based on the Negative Binomial distribution are commonly used, they lack the flexibility to independently characterize these dual sources of variability, thereby limiting their biological interpretability and personalization potential. Motivated by this shortcoming, we propose the Waring frailty model. Its structural properties allow for an explicit decomposition of variance, offering a principled way to distinguish individual-specific risk from contextual or environmental factors. This leads to a personalized cure rate, a critical feature in modern therapeutic areas such as immunotherapy, where patient response is highly heterogeneous. The model's performance is evaluated through a comprehensive Monte Carlo simulation study and is illustrated with an application to real colon cancer data. The results confirm that the Waring distribution, renowned in accident theory for variance decomposition, provides an effective and interpretable tool for cure rate estimation in survival analysis.

Keywords: frailty model, waring distribution, survival analysis, risk causes, variance decomposition, cure fraction

Volume 15 Issue 1 - 2026

Jonathan KJ Vasquez,¹ Vera LD Tomazella,²
Pedro Rafael D Marinho³

¹Institute of Mathematics and Computer Sciences, University of São Paulo, Brazil

²Department of Statistics, Federal University of São Carlos, Brazil

³Department of Statistics, Federal University of Paraíba, Brazil

Correspondence: Vera LD Tomazella, Department of Statistics, Federal University of São Carlos, São Carlos, SP, Brazil, Tel +5516981671390

Received: December 16, 2025 | **Published:** January 30, 2026

Introduction

Flexible cure rate modeling via discrete frailty under a minimum activation scheme¹ focuses on describing, in a biological scenario, the process by which patients may achieve a cure by considering the competition among multiple risk factors, such as initiated cells or pathological agents. In this formulation, the central element is the latent number of risk factors, treated as a discrete random variable representing discrete frailty and capturing individual heterogeneity with respect to the population baseline risk.

The approach was initially developed by Yakovlev et al.,² Yakovlev,³ and Tsodikov et al.,⁴ and is referred to as the “first activation scheme” (or “time minimums”). This approach offers a framework for modeling competing risks in survival analysis. A more in-depth explanation of the concepts and methodology of the competing causes model applied to survival data analysis in clinical epidemiology was provided by Nie et al.⁵ Similarly, do Nascimento et al.⁶ examined the impact of covariates on the causes of death in patients with sickle cell anemia. In this context, it is assumed that activation triggers the event of interest; that is, the first activation among all latent factors is decisive for the manifestation of the event.

Initially, without considering overdispersion or additional hierarchical structure, Yakovlev et al.² proposed the Poisson distribution to model this latent quantity, leading to the well-known promotion time model.⁷ In later works, the need to accommodate overdispersion led to considering a random Poisson mean following a gamma distribution, resulting in the Negative Binomial (NB)

distribution. However, although widely used, the NB does not adequately distinguish the intrinsic variability of patients (internal effect) from variability arising from unobserved factors (external effect), hindering a more precise decomposition of heterogeneity.

From this perspective, the Waring distribution⁸ emerges as a more appropriate alternative, as its mixture structure allows greater flexibility in modeling different heterogeneity levels associated with the number of risk factors. The Waring distribution clearly separates the internal effect, associated with inherent biological characteristics of the individual, and the external effect, associated with unobserved covariates influencing risk. Consequently, this approach promotes the personalization of the cure rate, making it especially suitable for clinical scenarios where individual response is determinant, as in modern oncological treatments.

Within this framework, discrete frailty stands out as a particularly suitable approach for representing unobserved heterogeneity in survival studies (Balakrishnan and Peng,⁸ Chen et al.,⁹ Tomazella,¹⁰ Hougaard,¹¹ Caroni et al.,¹² Vaupel et al.,¹³ Vasquez et al.,¹⁴). Unlike traditional continuous frailty distributions, discrete formulations allow the frailty term to take the value zero, enabling the explicit identification of individuals who are completely immune to the event of interest and, consequently, compatible with the presence of a cure fraction. This feature is especially relevant in modern clinical contexts, where therapeutic advances have produced groups of patients who remain event-free for extended periods of follow-up.

Furthermore, the discrete specification facilitates the biological interpretation of the number of risk factors accumulated by each

individual, naturally aligning with the hierarchical structures underlying Waring-based models (Rodrigues et al.,¹ Mota et al.,¹⁵ de Souza et al.,¹⁶ Vasquez et al.,¹⁷ Cancho et al.,¹⁸) Incorporating discrete distributions such as zero-modified power series families¹⁹ also increases modeling flexibility, allowing the framework to accommodate diverse patterns of variability arising from a higher prevalence of immune individuals, overdispersion, or internal mechanisms of risk activation.

Taken together, the hierarchical structure of the Waring distribution and the ability to employ discrete frailty provide a robust, interpretable, and biologically coherent framework for cure rate survival modeling, offering a more accurate representation of the complex underlying risk-generating processes.

The structure of this article is organized as follows: in Section 2, the Waring distribution and its hierarchical representation are briefly presented, highlighting their main properties. Then, in Section 3, the proposed model with Waring frailty under a minimum activation scheme is introduced. Section 4 describes a simulation study performed to evaluate the model's performance and the associated inferential procedure. In Section 5, the methodology is applied to a real dataset on colon cancer. Finally, in Section 6, final considerations are presented.

The waring distribution: a hierarchical framework for heterogeneity

We begin this section by discussing the Waring Series, a fundamental structure for deriving the Waring distribution.²⁰ This distribution can be interpreted as a generalization of the Yule–Simon distribution²¹ and, simultaneously, as a special case of the generalized Waring distribution when $k=1$.²² With two parameters, the Waring distribution has a relatively simple form and has therefore proven especially attractive in various research areas. Below, we present the Waring Series, which underpins its probabilistic properties and allows for understanding its role in modern statistical models.

$$\frac{1}{x-a} = \sum_{m=0}^{\infty} \frac{(a)_m}{(x)_{m+1}}, \quad m=0,1,\dots, \quad (1)$$

where $(\alpha)_q = \alpha(\alpha+1)\cdots(\alpha+q-1)$; if $\alpha > 0$ it follows that

$(\alpha)_q = \Gamma(\alpha+q)/\Gamma(\alpha)$. If $\rho = x - a$, the probability mass

function (p.m.f.) follows directly from (1)

$$p_m = P[M = m] = \rho \frac{(a)_m}{(a+\rho)_{m+1}}, \quad m = 0,1,2,\dots \quad (2)$$

where $\alpha > 0$, $\rho > 0$, (if $\rho < 2$, the distribution has infinite variance).

A classic and widely adopted way to define the Waring distribution is through its hierarchical representation. This seeks to explicitly distinguish between internal and external sources of variability.²³ Irwin proposed a three-stage framework in which different levels of uncertainty are organized in a systematic and interpretable way.

We can observe in Figure 1 the stochastic representation of the discrete distribution (M), highlighting its three sources of variability σ_1^2 , σ_2^2 and σ_3^2 that contribute to the observed overdispersion. These variability components characterize the variance decomposition structure associated with the Waring distribution, allowing a clearer interpretation of the mechanisms governing model heterogeneity, from which it follows that

$$M | a, \rho \sim \text{Waring}(a, \rho) \quad (3)$$

The mean of the Waring distribution is given by

$$E(M) = \frac{a}{\rho-1} = \mu \quad (4)$$

The Waring distribution is characterized by over dispersion, meaning that $E(M) < \text{Var}(M)$. The variance is given by

$$\sigma^2 = \text{Var}(M) = \frac{a}{\rho-1} + \frac{2a}{(\rho-1)(\rho-2)} + \frac{a^2\rho}{(\rho-1)^2(\rho-2)}$$

$$= \mu + \frac{2}{\rho-2}\mu + \frac{\rho}{\rho-2}\mu^2 \quad (5)$$

Random Effect External Effects External Effects

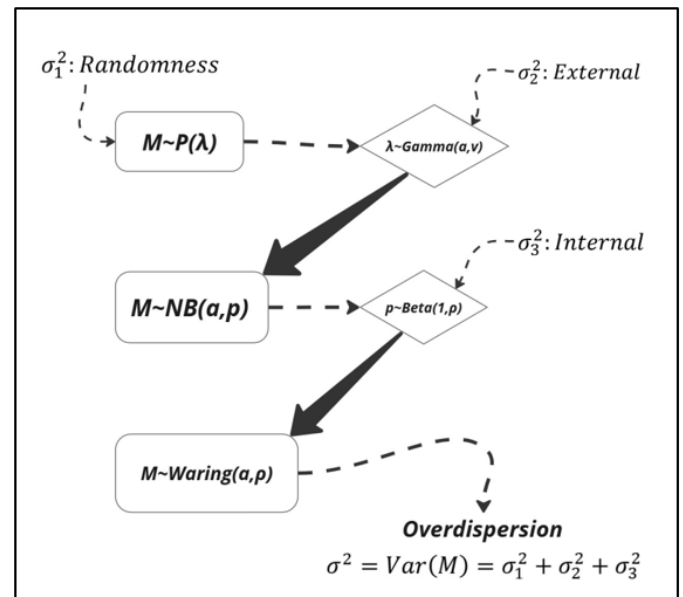


Figure 1 Hierarchical representation of the waring distribution.

Table 1 presents the decomposition of the total variance of the Waring distribution into three sources of variability: the random effect, the external effect, and the internal effect, with their respective variation rates.

Table 1 Variance decomposition of the waring distribution

Source of Variability	Variance	Variance rate (%)
Random Effect	$\sigma_1^2 = \mu$	$\frac{\rho-2}{\rho} \frac{1}{1+\mu}$
External Effect	$\sigma_2^2 = \frac{2}{\rho-2} \mu$	$\frac{2}{\rho} \frac{1}{1+\mu}$
Internal Effect	$\sigma_3^2 = \frac{\rho}{\rho-2} \mu^2$	$\frac{\mu}{1+\mu}$
Total	$\sigma^2 = \frac{\rho}{\rho-2} (\mu + \mu^2)$	1

Algorithm 1 Generate a sample from the waring (a, ρ) distribution

```

Require:  $n, \rho, a, x_1$ 
For  $i = 1$  to  $n$  do
   $p \leftarrow \text{Beta}(\rho, 1)$ 
   $\lambda \leftarrow \text{Gamma}\left(a_i, \text{shape} = a_i, \text{scale} = \frac{1-p}{p}\right)$ 
   $M[i] \leftarrow \text{Poisson}(\lambda)$ 
end for return  $M$ 

```

Algorithm 2 A generation of failure and censorship times

```

Require:  $n, M, a, \rho, \lambda$ 
For  $i = 1$  to  $n$  do
   $N[i] \leftarrow \text{Waring}(1, \rho, a)$ 
  if  $N[i] = 0$  then
     $te[i] \leftarrow -\infty$ 
  else
     $te[i] \leftarrow \min\left(\text{Exp}(\lambda_0)_1, \dots, \text{Exp}(\lambda_0)_{N[i]}\right)$ 
  end if
   $ce[i] \leftarrow \text{Uniform}(2, 5)$ 
   $y[i] \leftarrow \min(te[i], ce[i])$ 
   $status[i] \leftarrow \text{if else}(te[i] < ce[i], 1, 0)$ 
end for return  $(y, status)$ 

```

From Table 1, the random effect is linked to unobserved heterogeneity among individuals; the external effect pertains to environmental or contextual factors that influence the time to the event; and the internal effect captures changes associated with the mean survival time itself. When the mean survival time is low, the random effect explains the largest share of the variability, as increases, greater weight shifts to the internal effect, reflecting modifications in the overall risk structure. The contribution of the external effect occupies an intermediate position and depends on the parameter, which, as it increases, diminishes the relative importance of this component in the total variability.

Model specification with waring discrete frailty

This section formalizes the Waring discrete frailty model under a minimum activation scheme. In this framework, the event of interest

occurs upon the activation of the first one among a set of latent risk factors. This characterizes systems where a single triggering event is sufficient for failure, making the scheme particularly apt for modeling phenomena where exposure to an initial hazard leads to immediate consequences.

Within survival analysis, this approach models a competing risks scenario where an individual possesses M latent risk factors, with M being a discrete random variable. The event manifests when the earliest of these potential causes is activated, capturing the biological or clinical premise that the first active agent initiates the disease or failure process.

Let M be a random variable representing the number of risk factors or causes associated with the occurrence of the event of interest, with a probability distribution given by:

$$p_m = P[M = m], m = 0, 1, 2, \dots \quad (6)$$

Given $M = m$, let T_i , for $i = 1, 2, \dots, m$, be continuous and independent (non-negative) random variables, representing the time of occurrence or activation of the event of interest due to the i^{th} risk factor. The variables T_i are independent of M . The probability density function of T_i is denoted by $f_0(t_i)$, such that the cumulative distribution function (c.d.f.) of T_i is given by $F_0(t_i)$ the survival function by $S_0(t_i)$, and the associated risk function by $h_0(t_i)$.

We opted to use the notation $T = t$ instead of $T_i = t_i$ to simplify the representation. Thus, we consider $T_{(1)}, T_{(2)}, \dots, T_{(M)}$, where $T_{(1)} \leq T_{(2)} \leq \dots \leq T_{(M)}$ correspond to the first M order statistics of T_i . We emphasize that only the time $T_{(K)}$, with $K = 1, 2, \dots, M$, which triggers the mechanism, will be observed.

Here, K can be understood as an indicator of the individual's immune system capacity. When the event of interest occurs, the time until that occurrence is represented by the i^{th} statistic of order $T_{(K)}$. In the studies by Cooner et al.,^{24,25} and Rodrigues et al.,²⁶ the event manifests when K of the M possible causes are activated. Following this line of reasoning, we can explore three different configurations for K . In this context, considering the particular case where $K=1$ the observed time is $T_{(M)}$, indicating the activation of all risk factors.

$$T(M) = \begin{cases} Y = \min\{T_{(1)}, T_{(2)}, \dots, T_{(M)}\}, & \text{if } M \geq 1, \\ \infty, & \text{if } M = 0 \end{cases}$$

As indicated by Cooner et al.²⁵ and Rodrigues et al.,²⁶ the survival function under the minimum activation scheme is expressed by

$$\begin{aligned} S_p(t) &= G_M[S_0(t)] \\ &= \frac{\rho}{a+\rho^2} {}_2F_1(a, 1, a+1+\rho; S_0(t)), t > 0 \end{aligned} \quad (7)$$

where ${}_2F_1(a, 1, a+1+\rho; S_0(t))$ is the Gaussian hyper geometric function Irwin,⁷ and $\rho > 2$.

Given the survival function, $S_p(t)$, (7) we have that

$$\lim_{t \rightarrow \infty} S_p(t) = P[M = 0] = p_0 = \frac{\rho}{a+\rho}, \quad \rho > 2, \quad (8)$$

where p_0 is the proportion of “cured” or “immune” individuals that may be present in the population. An individual is considered immune if they are not subject to the event of interest, and their corresponding probability p_0 is the cure rate.

From (7), we can obtain its respective density function, given by

$$f_p(t) = -\frac{d}{dt} S_p(t) = f_0(t) \frac{ap}{(a+\rho)(a+\rho+1)} {}_2F_1(a+1, 2, a+\rho+2; S_0(t)) \quad (9)$$

Therefore, the hazard function is given by

$$h_p(t) = \frac{f_p(t)}{S_p(t)} = \frac{af_0(t)}{a+\rho+1} = \left(\frac{{}_2F_1(a+1, 2, a+\rho+2; S_0(t))}{{}_2F_1(a, 1, a+1+\rho; S_0(t))} \right) \quad (10)$$

$$L(\theta | D) = \prod_{i=1}^n \left[f_0(t_i) \frac{ap}{(a+\rho)(a+\rho+1)} {}_2F_1(a+1, 2, a+\rho+2; S_0(t_i)) \right]^{\delta_i} \left[\frac{a}{a+\rho} {}_2F_1(a, 1, a+1+\rho; S_0(t_i)) \right]^{1-\delta_i} \quad (11)$$

Therefore, its corresponding log-likelihood is

$$l(\theta) = \sum_{i=1}^n \left\{ \delta_i \log \left[f_0(t_i) \frac{ap}{(a+\rho)(a+\rho+1)} {}_2F_1(a+1, 2, a+\rho+2; S_0(t_i)) \right] + (1-\delta_i) \log \left[\frac{a}{a+\rho} {}_2F_1(a, 1, a+1+\rho; S_0(t_i)) \right] \right\} \quad (12)$$

where $\theta = (\rho, a)$, $D = \{(t_i, \delta_i), i=1, \dots, n\}$, $f_0(t_i)$ is the basis density function and $S_0(t_i)$ is the basis survival function.

The inclusion of covariates in the minimum activation model is achieved through an exponential link function applied to the parameter a , linking it to the linear predictor $x^\top \beta$. This specification ensures the positivity of the parameter a , and allows for a straightforward interpretation of the effects of covariates on the cure fraction. Here, $x^\top = (1, x_1, \dots, x_p)$ denotes the vector of observed covariates, while $\beta = (\beta_0, \beta_1, \dots, \beta_p)^\top$ represents the corresponding regression coefficients. Furthermore, the activation times Z_0, Z_1, \dots, Z_M are assumed to be independent and to follow an Exponential distribution with rate parameter $\lambda > 0$, leading to the model parameter vector $\theta = (\beta^\top, \rho, \lambda)$. In practical applications, the same set of covariates may simultaneously influence different components of the model.

Simulation study

A Monte Carlo simulation study for the model will be presented. Following this, Algorithm 1 is presented to generate samples from a Waring distribution, which is a consequence of the hierarchical representation presented in (3). In this algorithm, however, we only generate the number M_i of failure factors for the i^{th} individual, with $i = 1, \dots, n$. In applications, the value of M_i is a latent variable in our model.

Next, we detail the Algorithm 2 for generating failure and censoring times.

The study involved simulations with 1000 samples, considering the sizes $n = 100, 250, 500, 750, 1000$, fixing the value of $\rho = 4$, $\beta_0 = 2$ and $\beta_1 = -1$, with the covariate x_1 generated according to a Binomial (1, 0, 5) distribution. The censoring times were simulated from a uniform distribution in the interval [2, 5], so that approximately 50% of the data were censored. The times until the occurrence of the event of interest followed an exponential distribution with parameter $\lambda = 1$. This procedure aimed to investigate the performance of the proposed model under different sample sizes.

The simulation results, generated using code in the R Studio software, are presented in Figure 2

In the analysis of Figure 2, it can be observed that as the sample size increases, the mean of the maximum likelihood estimator becomes

Inference

The following presents the inferential methodology adopted for estimating the model parameters, using the maximum likelihood method. For its application, the expressions for the survival function (7) and the probability density function (9) are necessary. Thus, the maximum likelihood functions for the model are given by

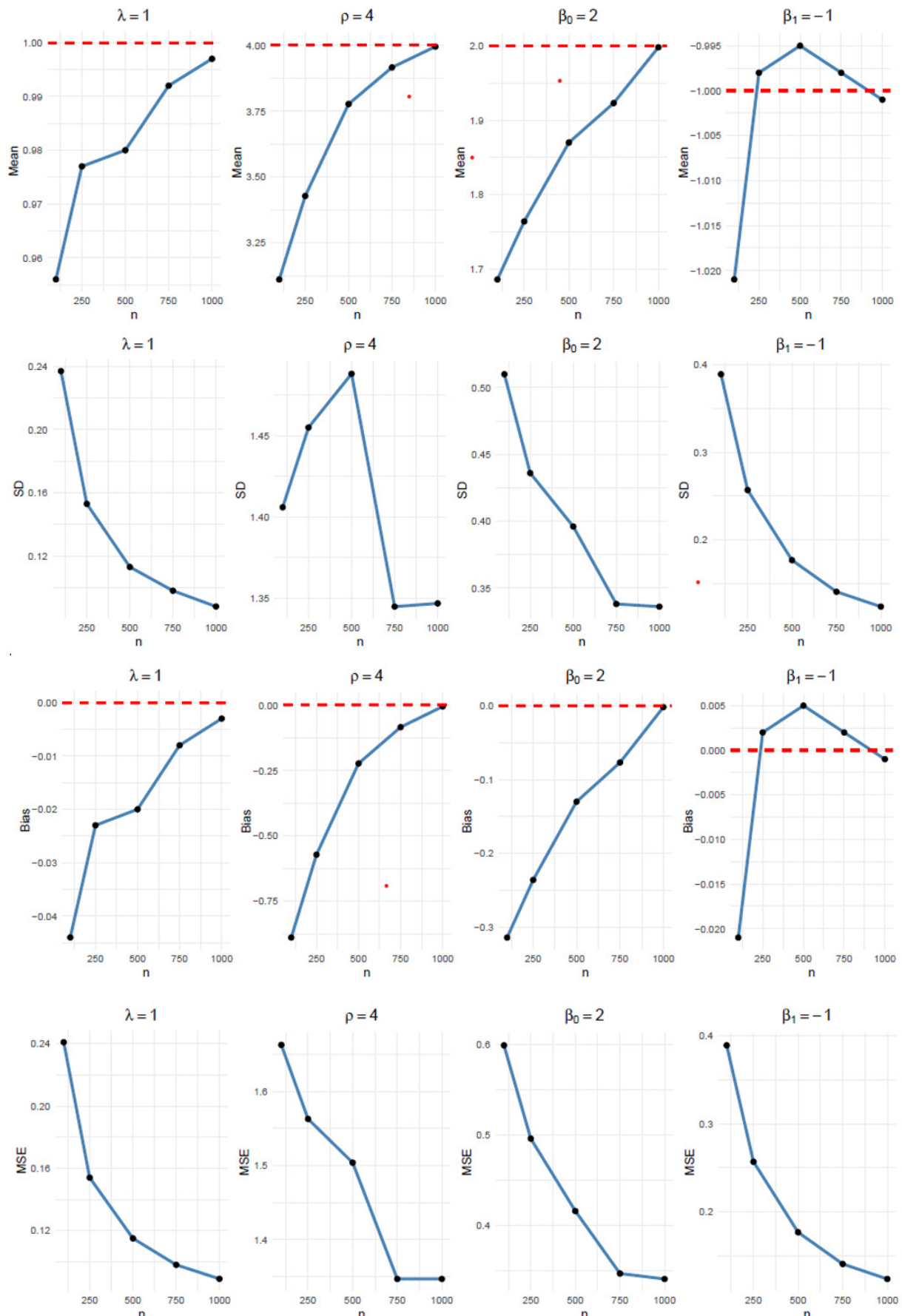
closer to the real values, indicating asymptotic consistency. The absolute bias decreases systematically, showing that the estimators are asymptotically unbiased, especially for ρ , whose high initial bias becomes almost zero with $n = 1000$. The standard deviations of the estimators decrease with increasing sample size, improving precision, although ρ shows relatively greater variability even in large samples. The mean squared error also decreases for all parameters, especially for λ , β_0 , and β_1 , reflecting a good balance between bias and variance. Furthermore, the confidence intervals show coverage proportions close to 95%, even in smaller samples, demonstrating good calibration of the estimators.

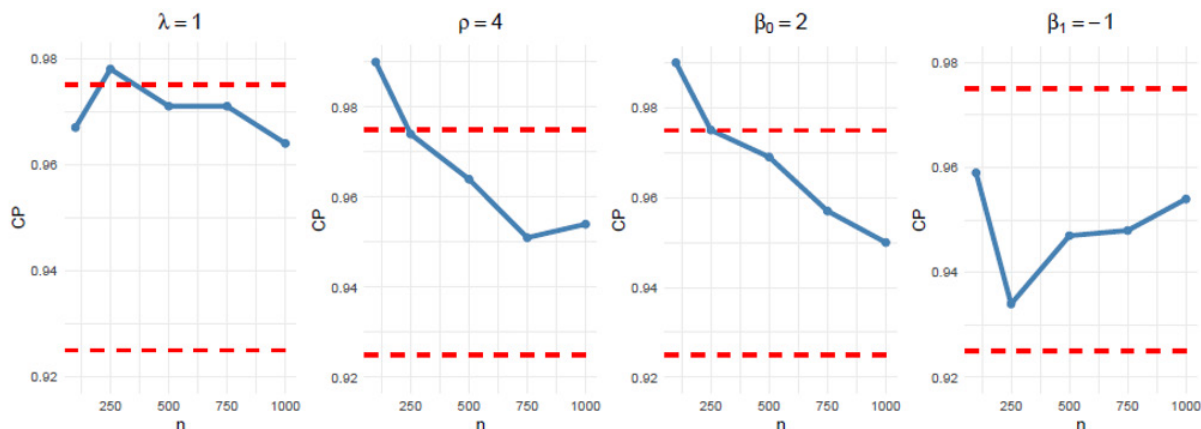
Application for real data

The dataset “colon”, available in the “survival” package of the R language, will be used. This database provides data from a multicenter clinical trial conducted to evaluate the efficacy of adjuvant chemotherapy in patients undergoing surgical resection of stage B or C colon cancer, according to the Dukes classification. The study, led by Moertel et al.,²⁷ compared three therapeutic strategies: a control group (observation only after surgery), levamisole administration, and a combination of levamisole with fluorouracil (5-FU), with the aim of assessing their impact on tumor recurrence and mortality.

The database contains information from 929 patients, each with up to two recorded observations: one regarding disease recurrence and the other regarding death, totaling 1,858 records. The collected information covers both demographic and clinical aspects of the individuals, allowing for robust analyses of time-to-event models, especially survival models with or without competing risks.

Regarding the status of the events, it is observed that approximately 50.5% of the observations correspond to censored data, while 49.5% indicate observed events, a proportion that ensures a good balance between events and censoring in the survival models that are intended to be used. The main variables available in the dataset are described in the Table 2.



**Figure 2** Mean, SD, Bias, MSE, and CP of the parameters as a function of sample size for simulated model data.**Table 2** Description of the covariates belonging to the colon cancer data

Covariate	Category	Description	n	%
X_1 : Age	-	$\mu = 60$, $\sigma = 11.95$	1858	-
X_2 : Treatment	0	Did not receive	630	33.90%
	1	Received	1028	66.10%
X_3 : Intestinal obstruction caused by the tumor	0	No	1498	80.62%
	1	Yes	360	19.38%
X_4 : Tumor attached to other structures	0	No	1588	85.47%
	1	Yes	270	14.53%
X_5 : More than four lymph nodes affected	0	No	1348	72.55%
	1	Yes	510	27.45%

Model adjustment considering the presence of covariates

We begin by analyzing the isolated effect of each covariate on the time to death of patients with *colon* cancer, considering the link function applied to the parameter a . The parameter estimates and the corresponding cure rates were obtained using the L-BFGS-B optimization method²⁸ and are presented below.

In the analysis of Table 3, it is observed that treatment is associated

with an increase in the cure fraction for treated patients, compared to those who were not treated, suggesting a beneficial effect of the intervention. On the other hand, the presence of intestinal obstruction caused by the tumor, tumor adherence to other structures, and involvement of four or more lymph nodes are related to lower chances of cure. This last covariate presented the greatest negative impact for patients with more than 4 positive lymph nodes, compared to the others.

Table 3 MLE, SE and CI(95%) obtained for the model according to the covariates treatment, intestinal obstruction caused by the tumor, Tumor adhered to other structures and presence of more than four compromised lymph nodes

Parameter	MLE	SE	CI 95%	
			Lower	Upper
ρ	2.944	1.266	0.463	5.426
λ	-2.006	0.138	-2.277	-1.735
α	1.478	0.071	1.340	1.617
β_{01} (intercept)	0.725	0.236	0.262	1.187
β_{11} (Treatment)	-0.280	0.093	-0.461	-0.098
p_{01} (No)	0.423	0.159	0.112	0.735
p_{11} (Yes)	0.492	0.147	0.204	0.781
AIC	5521.68			
BIC	5549.32			

Table 3 Continued....

ML	-2755.84				
ρ		3.248	1.613	0.087	6.409
λ		-1.982	0.143	-2.261	-1.702
α		1.470	0.071	1.330	1.610
β_{02} (intercept)		0.423	0.226	-0.020	0.866
β_{12} (Intestinal obstruction)		0.382	0.112	0.163	0.602
p_{02} (No)		0.486	0.156	0.181	0.792
p_{12} (Yes)		0.392	0.174	0.051	0.734
AIC		5519.20			
BIC		5546.83			
ML	-2754.60				
ρ		2.949	1.287	0.428	5.471
λ		-2.008	0.139	-2.282	-1.735
α		1.479	0.071	1.340	1.618
β_{03} (intercept)		0.481	0.227	0.036	0.925
β_{13} (Tumor attached)		0.401	0.122	0.163	0.639
p_{03} (No)		0.483	0.150	0.188	0.778
p_{13} (Yes)		0.385	0.167	0.059	0.712
AIC		5520.00			
BIC		5547.64			
ML	-2755.00				
ρ		4.078	2.488	-0.798	8.954
λ		-2.072	0.142	-2.351	-1.794
α		1.502	0.069	1.367	1.637
β_{04} (intercept)		0.082	0.204	-0.318	0.481
β_{14} (More than 4 lymph nodes)		1.302	0.100	1.106	1.498
p_{04} (No)		0.550	0.134	0.287	0.812
p_{14} (Yes)		0.249	0.206	-0.154	0.652
AIC		5356.33			
BIC		5383.96			
ML	-2673.16				

Next, in Figure 3, we observe strong evidence of a cure fraction for all covariates, with the model curves (dashed lines) fitting well with the Kaplan-Meier estimate (solid line), indicating a good fit of the

model to the melanoma data.

Table 4 shows the decomposition of the total variance of the Waring frailty model considering the different covariates.

Table 4 Decomposition of the variance of the Waring frailty model according to treatment, intestinal obstruction caused by the tumor, tumor adherent to other structures, and presence of more than four compromised lymph nodes

Source of variability	Treatment				Intestinal obstruction			
	No		Yes		No		Yes	
	Variance	VR	Variance	VR	Variance	VR	Variance	VR
Random Effect	2.06	0.11	1.56	0.12	1.53	0.15	2.24	0.12
External Effect	4.37	0.22	3.3	0.27	2.45	0.24	3.59	0.19
Internal Effect	13.27	0.67	7.59	0.61	6.07	0.61	13.04	0.69
No								
Yes								
Variance								
Random Effect	1.62	0.12	2.41	0.09	1.09	0.24	3.99	0.1
External Effect	3.41	0.26	5.09	0.2	1.04	0.24	3.84	0.1
Internal Effect	8.12	0.62	18.1	0.71	2.31	0.52	31.25	0.8

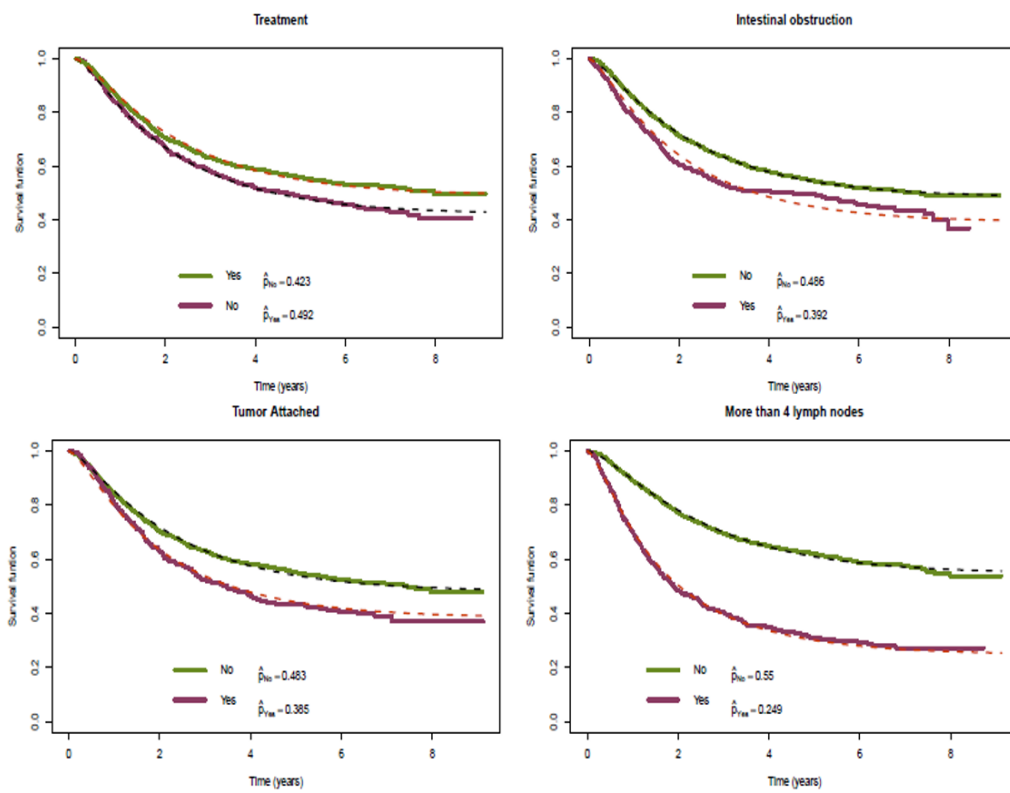


Figure 3 Kaplan-Meier estimate and waring frailty model survival curves for colon cancer dataset according to treatment, tumor-induced bowel obstruction, tumor adherence to other structures, and presence of more than four compromised lymph nodes.

In all groups, the highest rate of change (VR) is associated with the internal effect of the total variance. This result indicates that endogenous processes related to disease progression are primarily responsible for the observed variability. The external effect, associated with contextual or environmental factors, contributes less significantly, while the random effect, linked to unobserved individual heterogeneity, has a relatively smaller share. The highest RV for the internal effect was observed in the group with more than four affected lymph nodes, followed by the group with an adherent tumor, suggesting that in these subgroups the variability is strongly determined by factors intrinsic to the tumor progression process.

After analyzing each covariate individually, we now proceed to include all of them simultaneously in the model. As in the individual parameter estimation, the same estimation procedure was employed in this joint adjustment, using the L-BFGS-B optimization method²⁸ to obtain the parameter estimates

The Table 5 presents the parameter estimates of the fitted model with all covariates considered simultaneously. The structural parameters ρ , λ and α have confidence intervals that do not include zero, indicating statistical significance. Among the covariate coefficients, the intercept (β_0) is not statistically significant, given that its confidence interval includes zero.

Table 5 MLE, SE and CI (95%) obtained for the model considering all covariates together

Parameter	MLE	SE	CI 95%	
			Lower	Upper
ρ	3.091	0.964	1.201	4.981
λ	-2.164	0.11	-2.38	-1.948
α	1.539	0.059	1.424	1.655
β_0 (intercept)	0.119	0.288	-0.447	0.684
β_1 (Treatment)	-0.303	0.094	-0.488	-0.119
β_2 (Intestinal obstruction)	0.442	0.114	0.218	0.665
β_3 (Tumor attached)	0.423	0.124	0.18	0.666
β_4 (More than 4 lymph nodes)	1.342	0.101	1.144	1.54
β_5 (Age)	0.002	0.004	-0.005	0.009

The treatment (β_1) showed a significant negative effect, suggesting a higher probability of cure among treated patients. However, adverse clinical variables such as intestinal obstruction (β_2), tumor adherent to other structures (β_3), and the presence of more than four compromised lymph nodes (β_4) showed positive and statistically significant effects, indicating a worse prognosis for patients with these conditions. Finally, age (β_5) did not show a significant effect,

suggesting that, in this model, age does not significantly influence the cure rate.

Table 6 shows the influence of the covariates age, treatment, intestinal obstruction, adherent tumor and +4 lymph nodes, on the cure rate (p_0) and on the rate of change of the internal effect (RCIE).

Table 6 p_0 and RCIE of patients with influence of all covariates in the proposed model

Age	Treatment	Intestinal obstruction	Tumor attached	+4 lymph	RCIE
20	No	No	No	No	0.558 0.54
			Yes	Yes	0.25 0.818
		Yes	No	No	0.452 0.641
			Yes	Yes	0.178 0.873
			No	No	0.448 0.646
			Yes	Yes	0.175 0.875
	Yes	Yes	No	No	0.347 0.736
			Yes	Yes	0.122 0.914
		No	No	No	0.631 0.464
			Yes	Yes	0.309 0.768
			No	No	0.528 0.569
			Yes	Yes	0.226 0.835
60	No	Yes	No	No	0.523 0.574
			Yes	Yes	0.223 0.837
		No	No	No	0.418 0.673
			Yes	Yes	0.158 0.887
			No	No	0.538 0.559
			Yes	Yes	0.233 0.829
		Yes	No	No	0.433 0.66
			Yes	Yes	0.166 0.881
			No	No	0.428 0.664
			Yes	Yes	0.164 0.883
60	Yes	Yes	No	No	0.329 0.751
			Yes	Yes	0.114 0.92
		No	No	No	0.612 0.484
			Yes	Yes	0.292 0.782
			No	No	0.508 0.589
			Yes	Yes	0.213 0.846
		No	No	No	0.503 0.593
			Yes	Yes	0.209 0.848
			No	No	0.399 0.69
			Yes	Yes	0.148 0.895

We can observe that, regardless of age or treatment, the presence of adverse clinical factors such as intestinal obstruction, tumor adherence

to adjacent structures, and more than four compromised lymph nodes is associated with a significant reduction in the cure fraction and an increase in RCIE (transient ischemic attack). For example, for a 20-year-old patient without treatment and with all other adverse conditions present, the cure fraction drops to 0.122, with a high TVEI of 0.914, reflecting high intrinsic variability in disease progression. On the other hand, young treated individuals without adverse conditions have a higher probability of cure and lower RCIE, indicating a more favorable prognosis and less influence of internal variability. Age, by itself, shows a discrete impact, with a slight reduction in cure rates and an increase in RCIE when comparing patients aged 20 and 60 under

the same conditions. Treatment, in all scenarios, is associated with higher cure rates and lower RCIE values, reinforcing its protective role. Thus, the table shows that the patient's prognosis depends on a combination of the presence of unfavorable clinical conditions, age, and therapeutic intervention, with the internal effect being more pronounced in the most severe profiles.

Next, in Figure 4, the rates of change associated with the components of the Waring frailty model are presented, based on data from the Colon study and considering all covariates included in the analysis.

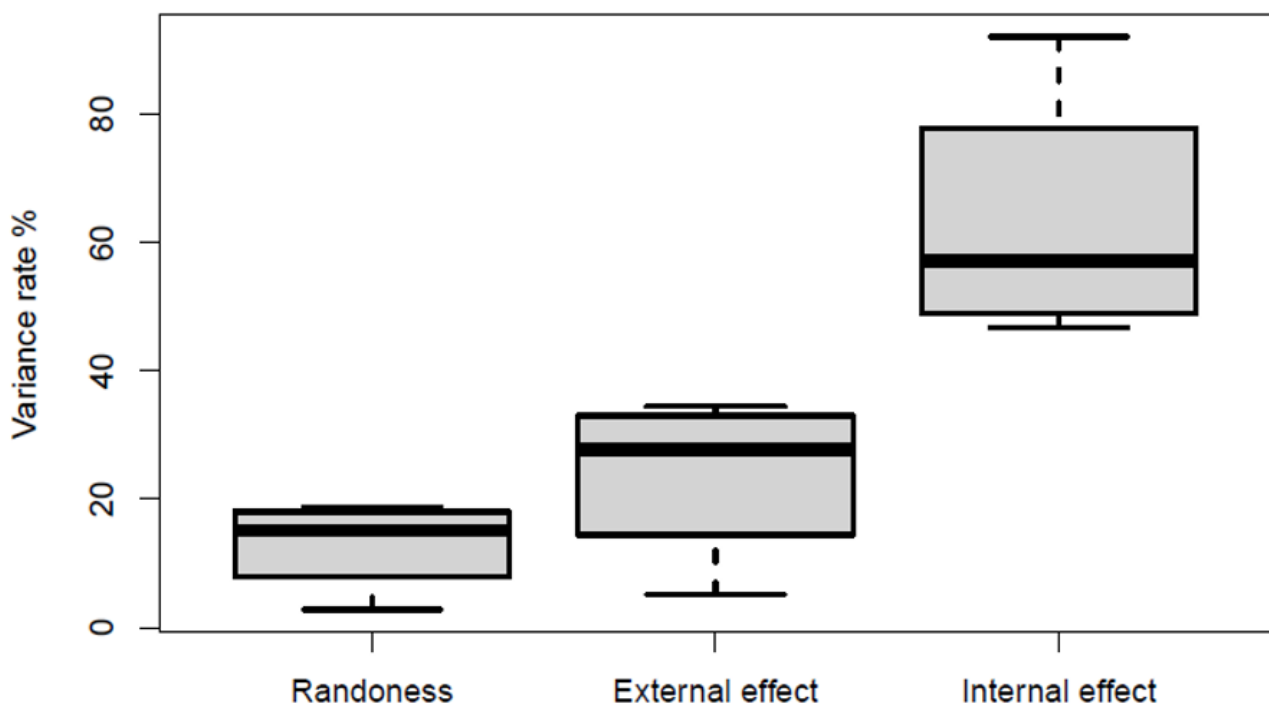


Figure 4 Sources of variability influenced by all covariates in waring's frailty model for colon cancer dataset.

It is observed that the internal effect is the main source of variability, with an average of 62.0%, indicating that a large part of the heterogeneity in patient survival is related to the disease's own evolutionary process over time. The external effect, associated with environmental and contextual factors, represents approximately 24.6% of the total variation, highlighting its relevance in explaining the model. On the other hand, the random effect, linked to unobserved individual heterogeneity, contributes only 13.4%, suggesting a more limited impact. These results highlight that most of the variability observed in the Colon study sample stems from structural components, especially the internal effect, which reinforces the importance of models that adequately capture the temporal dynamics of survival.

Final remarks

In this work, we present a frailty model with a minimal activation scheme that employs a discrete structure to represent the latent factors underlying the risk process. This approach provides a clear and interpretable depiction of how these factors accumulate among individuals and contribute to the observed variability in survival times. The model allows for the decomposition of this variability into three fundamental components: the random effect inherent to the process, the external effect associated with unobserved factors, and the internal effect linked to each patient's intrinsic characteristics. This decomposition, grounded in the stochastic representation of the Waring distribution, offers a more comprehensive understanding of population heterogeneity.

Furthermore, we conducted a simulation study to assess the model's performance across different scenarios, confirming its ability to accurately recover parameters and reliably identify sources of variability. The application of the model to real colon cancer data demonstrated its capacity to capture relevant patterns in the risk

process that traditional approaches fail to explain. These results highlight the potential of the proposed methodology as a robust tool for survival analyses requiring explicit assessment of heterogeneity and identification of the structural mechanisms influencing risk.

Acknowledgments

The second author gratefully acknowledges the financial support provided by the São Paulo Research Foundation (FAPESP), grant number 2024/23079-6, and by the Brazilian National Council for Scientific and Technological Development (CNPq), grant number 301941/2025-4.

Conflicts of interest

The authors declares that there are no conflicts of interest.

References

1. Rodrigues J, Castro M, Cancho VG, et al. COM-Poisson cure rate survival models and an application to a cutaneous melanoma data. *J Stat Plan Inference*. 2009;139:3605–3611.
2. Yakovlev AY, Tsodikov AD, Bass L. A stochastic model of hormesis. *Math Biosci*. 1993;116(2):197–219.
3. Yakovlev AY. Threshold models of tumor recurrence. *Math Comput Model*. 1996;23(6):153–164.
4. Tsodikov AD, Yakovlev AY, Asselain B. *Stochastic models of tumor latency and their biostatistical applications*. Vol 1. World Scientific; 1996.
5. do Nascimento EM, de Castro Lobo CL, de Bragança Pereira B, et al. Survival probability in patients with sickle cell anemia using the competitive risk statistical model. *Mediterr J Hematol Infect Dis*. 2019;11(1).
6. Chen MH, Ibrahim JG, Sinha D. A new Bayesian model for survival data with a surviving fraction. *J Am Stat Assoc*. 1999;94(447):909–919.

7. Irwin JO. The generalized Waring distribution. Part I. *J R Stat Soc A*. 1975;138(1):18–31.
8. Balakrishnan N, Peng Y. Generalized gamma frailty model. *Stat Med*. 2006;25(16):2797–2816.
9. Chen P, Zhang J, Zhang R. Estimation of the accelerated failure time frailty model under generalized gamma frailty. *Comput Stat Data Anal*. 2013;62:171–180.
10. Tomazella VLD. Modelagem de dados de eventos recorrentes via processo de Poisson com termo de fragilidade. PhD thesis. Universidade de São Paulo; 2003.
11. Hougaard P. Life table methods for heterogeneous populations: distributions describing the heterogeneity. *Biometrika*. 1984;71(1):75–83.
12. Caroni C, Crowder M, Kimber A. Proportional hazards models with discrete frailty. *Lifetime Data Anal*. 2010;16:374–384.
13. Vaupel JW, Manton KG, Stallard E. The impact of heterogeneity in individual frailty on the dynamics of mortality. *Demography*. 1979;16(3):439–454.
14. Vasquez JK, Molina KC, Tomazella V, et al. Multistate models with nested frailty for lifetime analysis: application to bone marrow transplantation recovery patients. *Commun Stat Theory Methods*. 2024;1–19.
15. Mota A, Milani EA, Calsavara VF, et al. Weighted Lindley frailty model: estimation and application to lung cancer data. *Lifetime Data Anal*. 2021;27(4):561–587.
16. de Souza D, Cancho VG, Rodrigues J, et al. Bayesian cure rate models induced by frailty in survival analysis. *Stat Methods Med Res*. 2017;26(5):2011–2028.
17. Vasquez JK, Rodrigues J, Balakrishnan N. A useful variance decomposition for destructive Waring regression cure model with an application to HIV data. *Commun Stat Theory Methods*. 2022;51(20):6978–6989.
18. Cancho VG, Macera MA, Suzuki AK, et al. A new long-term survival model with dispersion induced by discrete frailty. *Lifetime Data Anal*. 2020;26:221–244.
19. Molina KC, Calsavara VF, Tomazella VD, et al. Survival models induced by zero-modified power series discrete frailty: application with a melanoma data set. *Stat Methods Med Res*. 2021;30(8):1874–1889.
20. Rodríguez-Avi J, Conde-Sánchez A, Sáez-Castillo A, et al. A new generalization of the Waring distribution. *Comput Stat Data Anal*. 2007;51(12):6138–6150.
21. Yule GU. An introduction to the theory of statistics. *Bull Am Math Soc*. 1924;30:465–466.
22. Irwin JO, et al. The place of mathematics in medical and biological statistics. *J R Stat Soc*. 1963;126(Pt 1):1–41.
23. Irwin JO. The generalized Waring distribution applied to accident theory. *J R Stat Soc A*. 1968;131(2):205–225.
24. Cooner F, Banerjee S, Carlin BP, et al. Flexible cure rate modeling under latent activation schemes. *J Am Stat Assoc*. 2007;102(478):560–572.
25. Cooner F, Banerjee S, McBean AM. Modelling geographically referenced survival data with a cure fraction. *Stat Methods Med Res*. 2006;15(4):307–324.
26. Rodrigues J, Cancho VG, de Castro M, et al. On the unification of long-term survival models. *Stat Probab Lett*. 2009;79(6):753–759.
27. Moertel CG, Fleming TR, Macdonald JS, et al. Levamisole and fluorouracil for adjuvant therapy of resected colon carcinoma. *N Engl J Med*. 1990;322(6):352–358.
28. R Core Team. *R: a language and environment for statistical computing*. Vienna, Austria; 2018.